



Article

Interpolating Hydrologic Data Using Laplace Formulation

Tianle Xu, Venkatesh Merwade and Zhiquan Wang

Special Issue

Remote Sensing and GIS Technology Applications for Water Resources and Flood Risk Management in River Basin and Coastal Zones

Edited by

Dr. Pierfranco Costabile, Dr. John Kalogiros, Prof. Dr. Venkatesh Merwade and Dr. Jochen E. Schubert









Article

Interpolating Hydrologic Data Using Laplace Formulation

Tianle Xu¹, Venkatesh Merwade ^{1,*} and Zhiquan Wang ²

- ¹ Lyles School of Civil Engineering, Purdue University, West Lafayette, IN 47907, USA; xu1361@purdue.edu
- Department of Computer Science, Purdue University, West Lafayette, IN 47907, USA; wang4490@purdue.edu
- * Correspondence: vmerwade@purdue.edu

Abstract: Spatial interpolation techniques play an important role in hydrology, as many point observations need to be interpolated to create continuous surfaces. Despite the availability of several tools and methods for interpolating data, not all of them work consistently for hydrologic applications. One of the techniques, the Laplace Equation, which is used in hydrology for creating flownets, has rarely been used for data interpolation. The objective of this study is to examine the efficiency of Laplace formulation (LF) in interpolating data used in hydrologic applications (hydrologic data) and compare it with other widely used methods such as inverse distance weighting (IDW), natural neighbor, and ordinary kriging. The performance of LF interpolation with other methods is evaluated using quantitative measures, including root mean squared error (RMSE) and coefficient of determination (R²) for accuracy, visual assessment for surface quality, and computational cost for operational efficiency and speed. Data related to surface elevation, river bathymetry, precipitation, temperature, and soil moisture are used for different areas in the United States. RMSE and R² results show that LF is comparable to other methods for accuracy. LF is easy to use as it requires fewer input parameters compared to inverse distance weighting (IDW) and Kriging. Computationally, LF is faster than other methods in terms of speed when the datasets are not large. Overall, LF offers a robust alternative to existing methods for interpolating various hydrologic data. Further work is required to improve its computational efficiency.

Keywords: spatial interpolation; hydrologic data; Laplace equation; IDW; natural neighbor; ordinary kriging



Citation: Xu, T.; Merwade, V.; Wang, Z. Interpolating Hydrologic Data Using Laplace Formulation. *Remote Sens.* **2023**, *15*, 3844. https://doi.org/10.3390/rs15153844

Academic Editor: Chung-yen Kuo

Received: 17 May 2023 Revised: 20 July 2023 Accepted: 29 July 2023 Published: 2 August 2023



Copyright: © 2023 by the authors. Licensee MDPI, Basel, Switzerland. This article is an open access article distributed under the terms and conditions of the Creative Commons Attribution (CC BY) license (https://creativecommons.org/licenses/by/4.0/).

1. Introduction

Accurate simulation of hydrologic processes is essential for addressing various societal issues related to water management, flood forecasting, and agricultural production. The spatial description of natural variables, including topography, precipitation, temperature, and soil moisture, plays a crucial role in hydrologic simulations. For instance, precipitation drives the hydrologic cycle, and an accurate representation of its spatial pattern and dynamics is necessary for reliable simulations [1,2]. Soil moisture representation affects the partitioning of rainfall into infiltration and direct runoff [3–5]. Topography influences the representation of the stream network and other watershed characteristics, such as slope and flow length, which impact water movement on the surface [6,7]. Climate variables such as temperature and relative humidity are essential for estimating evaporation and evapotranspiration [8]. While continuous topographic datasets are often available for many regions, continuous weather datasets, including rainfall, soil moisture, and temperature, are primarily derived from satellite imagery or simulation models and may not be as accurate as ground observations [9–14]. Therefore, spatial interpolation of ground data, where available, is preferred for hydrologic applications at the watershed scale.

Spatial interpolation methods are actively researched for rainfall due to their critical role as the primary input to hydrologic models [15–19]. This research is primarily driven by the need to accurately represent the spatio-temporal dynamics of rainfall from a limited number of ground observations under multiple geographic and topographic

Remote Sens. 2023, 15, 3844 2 of 19

conditions [17,20,21]. Deterministic methods such as Inverse Distance Weighting (IDW) and Thiessen polygons are commonly used due to their simplicity, while Kriging and its variants are widely employed as geostatistical approaches for rainfall interpolation. However, the performance of these methods varies depending on the spatial and temporal scale of the data and the topography of the region [15,22,23]. In certain situations, advanced techniques that combine multiple data sources (e.g., ground observations and satellite products) and interpolation methods are utilized to improve accuracy [24–26].

Interpolation methods for temperature data have been widely studied, with various approaches explored. These include simple methods such as IDW and natural neighbor [27–29], as well as more sophisticated techniques such as Kriging and co-kriging [28,30]. Regression-based methods, such as geographically weighted regression, have also been utilized [31,32]. Soil moisture is another variable commonly interpolated in hydrologic applications. Chen et al. [15] compared four different approaches for soil moisture interpolation in southwest China and determined that IDW was the most suitable method for their study area. However, the interpolation of soil moisture is also influenced by the terrain characteristics of the region. In situations involving complex terrain, hybrid regression kriging has been shown to produce optimal soil moisture interpolations [33].

In addition to rainfall, temperature, and soil moisture, other datasets, such as river bed elevations, require interpolation at a much finer spatial resolution. Various studies have been conducted to explore different interpolation methods for the construction of riverbed terrain [34–38]. These datasets are unique because they exhibit anisotropic characteristics and are available in different spatial configurations, including cross-sections, sparsely arranged irregular points from boat surveys, or gridded sets from multi-beam surveys. Merwade et al. [36] introduced elliptical inverse distance weighting (EIDW) as a method to account for anisotropy in bathymetry data, and it was found to be more accurate than other complex methods such as Kriging. In the case of larger rivers, simple methods such as inverse distance weighting (IDW) can also yield satisfactory results for generating riverbed surfaces [38]. However, even at smaller scales, the interpolation of river bathymetry is influenced by factors such as river size and geometry. Consequently, different methods have been reported to have superior performance depending on the specific characteristics of the dataset and the interpolation requirements. These methods include regression-kriging (RK) [35], Topo to Raster (TopoR) [34], Radial basis function (RBF), and the anisotropic form of ordinary kriging [37].

Existing literature demonstrates that no single method consistently works for every variable used in hydrologic applications, and their performance varies geographically. Complex methods such as Kriging and spline are not easily implemented, and many methods require multiple input parameters, which are subjectively selected [39]. Given these considerations, this study aims to explore a simpler approach to interpolating hydrologic data and evaluate its performance in comparison to widely used methods. Specifically, the focus of this investigation is on the utilization of the Laplace formulation [30–42] as a means of interpolating data used in hydrologic applications, referred to hereafter as hydrologic data. Traditionally employed in groundwater hydrology to establish a network of equipotential and flow lines, known as flownets, the Laplace formulation has previously demonstrated its effectiveness in studies conducted by Hess [43] and Lai [44] for estimating tidal constituents and river channel streamlines, respectively. This investigation seeks to extend and assess the broader applicability of the Laplace formulation for interpolating hydrologic variables.

The objectives of this study are as follows:

- 1. To apply the Laplace formulation for interpolating topography, climate, and soil data at multiple locations within the United States.
- 2. To compare the performance of the Laplace formulation with commonly used interpolation methods, including inverse distance weighting, natural neighbor, and ordinary kriging, in terms of accuracy, computational speed, and ease of implementation.

Remote Sens. 2023, 15, 3844 3 of 19

The primary contribution of this work is to propose a very simple approach, Laplace Formulation, for interpolation. The novelty of this approach lies in its simplicity because, unlike other methods, it does not use distance/area-based weights or high-order polynomials for interpolation.

2. Materials and Methods

2.1. Interpolation Methods

This section briefly describes the methods used for interpolating the data used in this study, with more details provided for the application of the Laplace formulation.

2.1.1. Inverse Distance Weighting (IDW)

The IDW interpolation method assumes that the influence of sampled points on estimates at an unsampled point decreases with distance [45]. The value at an unsampled point, therefore, can be determined using an inverse distance weighted average of a set of sample points within a circle of neighborhood with a defined search radius (Figure 1a) according to Equation (1).

$$\hat{z}_j = \sum_{i=1}^n w_i z_i \tag{1}$$

$$w_{i} = \frac{\frac{1}{d_{i}^{p}}}{\sum_{i=1}^{n} \left(\frac{1}{d_{i}^{p}}\right)}$$
 (2)

where z_i (i = 1, 2, ..., N) is observed value at a sample point i, d_i is the distance between the ith sampled point (z_i) and the unsampled point (z_j) and the parameter p is the weight parameter as an exponent to the distance. The larger the power, the stronger the weight of nearby points, so defining a higher value for power leads to less influence for points farther away.

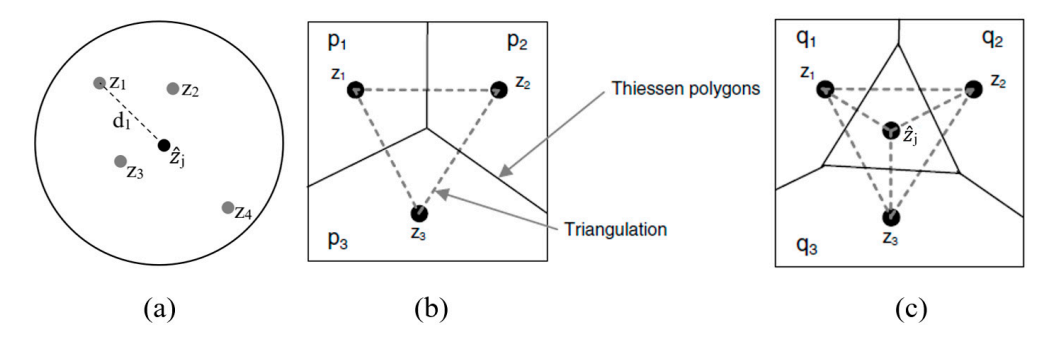


Figure 1. (a) IDW with a circular neighborhood; (b) natural neighbor with Thiessen polygon network; (c) natural neighbor with Thiessen polygons after insertion of point z_i [36].

2.1.2. Natural Neighbor

Natural neighbor provides estimates at unsampled points by giving weights to surrounding input sampled points according to the proportionate areas of Theissen/Voronoi polygons [46]. Thus, weights in natural neighbor interpolation are based on areas of Thiessen polygons. If there is a Voronoi diagram constructed based on some sample points $(z_1, z_2, ..., z_n)$, represented by the Thiessen/Voronoi polygons shown in Figure 1b, an unsampled point (z_j) inserted into the dataset will cause the voronoi diagram areas of the sample points to be reduced (Figure 1c). If p_i and q_i are the Voronoi diagram areas of the sample points z_i before and after the insertion of z_j , the weight for the sample point z_i is given by:

Remote Sens. 2023, 15, 3844 4 of 19

$$w_i = \frac{p_i - q_i}{p_i} \tag{3}$$

Once the weight is determined, Equation (1) is used by natural neighbor to predict the value of z_i .

2.1.3. Ordinary Kriging

Kriging is a geostatistical method that uses spatial correlation between sample points to interpolate values at unsampled points [47]. It is similar to IDW in that it also uses weights, but these are not based on the inverse distance between the sampled and unsampled points. Instead, weights are computed based on the statistical relationship between the sampled points.

The weight for each point is decided under the condition that the estimation variance:

$$\sigma^2_{E} = var(\hat{z}_i - z_i) \tag{4}$$

is minimum and that the interpolation is unbiased, which is warranted with unit sum weights:

$$\sum_{i=1}^{n} w_i = 1 \tag{5}$$

$$E[\hat{z}_j - z_j] = 0 \tag{6}$$

where E[] is the expectation operator. Ordinary kriging assumes the model:

$$z = \mu + \varepsilon \tag{7}$$

where z is the measured value, the constant mean (μ) is unknown, ϵ is a zero mean representing the variation around the mean with the existing semivariogram $\gamma(h)$ [48]. The estimator z_j can be expressed as Equation (1) if weight values (w_i) are determined for each sampled point.

It is assumed that the datasets are part of a realization of an intrinsic random function with an empirical semivariogram $\gamma(h)$ that helps to quantify the spatial correlation between measured points. Several functions (e.g., circular, spherical, exponential, and linear) are available to choose from for modeling the empirical semivariogram. In this study, the most commonly used spherical model [49] is fitted to the semivariogram as given by the following equation:

$$\gamma(h) = \begin{cases} c_0 + c \left(\frac{3h}{2a} - \frac{1}{2} \left(\frac{h^3}{a^3}\right)\right) & 0 < h \le a \\ c_0 + c & h > a \\ 0 & h = 0 \end{cases}$$
 (8)

where h is the lag vector, c_0 is the nugget, c is the partial sill value, and a is the range of the model.

2.1.4. Laplace Formulation

The Laplace equation is used to describe steady-state situations that are independent of time. In hydrology, a two-dimensional steady-state flow through a saturated, isotropic porous medium can be described by the Laplace Equation, as shown below.

$$\frac{\partial^2 h}{\partial x^2} + \frac{\partial^2 h}{\partial y^2} = 0 \tag{9}$$

where h is the hydraulic head, and x and y indicate the coordinates of the point in the flow field. Equation (9) can be solved to get a function h(x, y) that will give the value of hydraulic head h at any point in a two-dimensional flow region. This solution can also be

Remote Sens. 2023, 15, 3844 5 of 19

used to present a two-dimensional groundwater system with equipotential surfaces and corresponding flowlines, which together are referred to as the flow net.

The Laplace equation can be solved by analytic solutions that are exact. However, their complexity and the limitation that solutions are available only for simple boundary conditions make this method less practical [50]. Numerical methods are widely used for solving these equations. If the errors of approximation from a computer solution are acceptable, powerful computers and software are able to compute the results effectively. The numerical methods to solve the Laplace equation rely on the discretization of the flow field, where the flow region is divided into a finite number of blocks, as shown in Figure 2a. Each block has its own hydrogeologic properties and has a node at the center at which the hydraulic head is defined for the entire block. Consider one interior node and its neighbors, as shown in Figure 2a. Assuming the length of the side of each block in the y direction is Δy and that in the x direction is Δx , the hydraulic gradient (slope) between points (i -1, j) and (i, j) is:

$$\frac{\partial h}{\partial x} = \frac{h_{i-1,j} - h_{i,j}}{\Delta x} \tag{10}$$

where $h_{i,j}$ and $h_{i-1,j}$ are the hydraulic heads for each block. The hydraulic gradient between points (i+1, j) and (i, j) is:

$$\frac{\partial h}{\partial x} = \frac{h_{i,j} - h_{i+1,j}}{\Delta x} \tag{11}$$

Therefore, the differential of hydraulic gradient in the x direction is:

$$\frac{\partial^2 h}{\partial x^2} = \left(\frac{h_{i-1,j} - h_{i,j}}{\Delta x} - \frac{h_{i,j} - h_{i+1,j}}{\Delta x}\right) \frac{1}{\Delta x} = \frac{h_{i-1,j} - 2h_{i,j} - h_{i+1,j}}{(\Delta x)^2}$$
(12)

Similarly, the differential of hydraulic gradient in the y direction is:

$$\frac{\partial^2 h}{\partial y^2} = \frac{h_{i,j-1} - 2h_{i,j} - h_{i,j+1}}{(\Delta y)^2}$$
 (13)

According to the Laplace equation, the sum of Equations (12) and (13) leads to:

$$\frac{h_{i-1,j} - 2h_{i,j} - h_{i+1,j}}{(\Delta x)^2} + \frac{h_{i,j-1} - 2h_{i,j} - h_{i,j+1}}{(\Delta y)^2} = 0$$
(14)

If $\Delta x = \Delta y$, then

$$h_{i,j} = \frac{1}{4} (h_{i,j+1} + h_{i+1,j} + h_{i,j-1} + h_{i-1,j})$$
(15)

In summary, the hydraulic head at any node is the average of its four surrounding values. For points along the boundary, such as point (i, j) in Figure 2b, the value of the point above point (i, j), which is an imaginary point, is the same as that of point (i, j - 1). Thus,

$$h_{i,j} = \left(2h_{i,j-1} + h_{i+1,j} + h_{i-1,j}\right)/4 \tag{16}$$

For a corner point such as point (i, j) in Figure 2c, its value is the average of four surrounding points, and the value of an imaginary point at the left side and above the point (i, j) would be the same as points (i, j - 1) and (i + 1, j), respectively.

$$h_{i,j} = (2h_{i,j-1} + 2h_{i+1,j})/4 (17)$$

To generalize the application of the Laplace formulation for interpolation, h in the above equations can be replaced with the variable of interest, including elevation, temperature, precipitation, and soil moisture. The application of Laplace interpolation is described by considering a simple example with scatter measurements of variable z, as shown in Figure 2d. Let us assume that these measurements need to be interpolated to create a raster

Remote Sens. 2023, 15, 3844 6 of 19

or grid with a value in each cell, as shown in Figure 2e. If one or more measurements fall within a cell, that cell gets the average value of those measurements (clear cells), and all other cells are assigned an initial value of zero (shaded cells), as shown in Figure 2f. If the nodal grid has N unmeasured nodes (zero cells), it is possible to produce N linear, algebraic equations in N unknowns. To solve these N equations effectively, an iterative process called the relaxation method [51] is used.

Each internal cell's value with a zero value (shaded cell) is computed by taking the average of its four neighboring cells (Equation (15)). Equations (16) and (17) are used to compute values for shaded cells along the boundary. In the first iteration, Equations (15)–(17) are used to compute values for all unknown cells. Equations (15)–(17) are solved again for all unknown cells (next iteration), and the new values are compared with the previous values. If the difference between the new value and the previous value (residual) is greater than the specified threshold, the iterations will continue until the residual is less than or equal to the specified threshold, as shown in Figure 3. Consider the highlighted cell, which gets a value of 5 in the second iteration, 7.13 in the next iteration. Finally, it attains a value of 9.64 after several iterations to get a residual of 0.47, which is less than the specified threshold of 1.

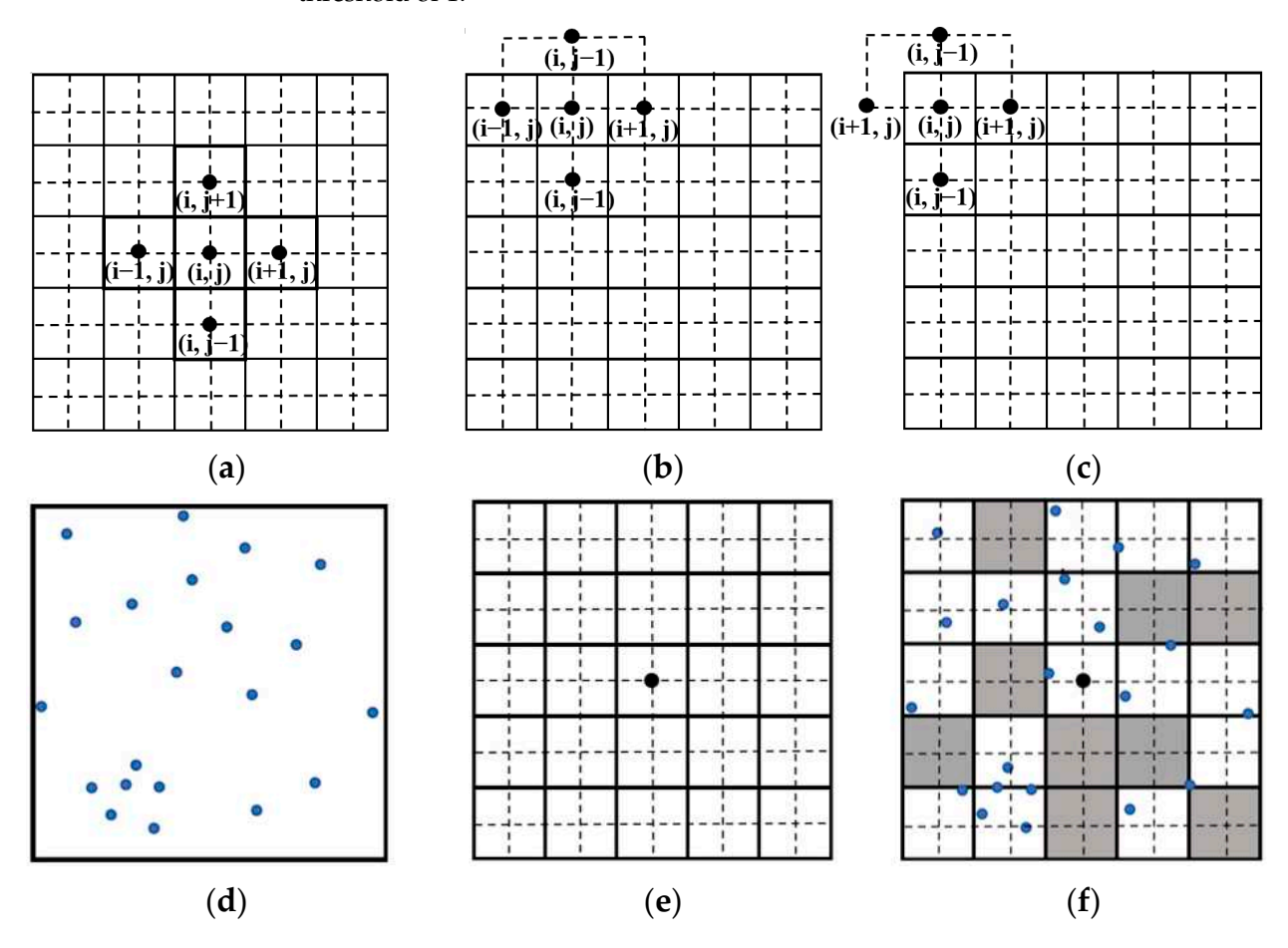


Figure 2. Hypothetical flow region showing: (a) Laplace equation application at internal nodes; (b) Laplace equation application at the boundary; (c) Laplace equation application at the corner; (d) scatter measures; (e) grid with center nodes; (f) scatter points interpolated in the grid.

Remote Sens. 2023, 15, 3844 7 of 19

	6	10	11	0	12	Sample grid with elevation
	3	7	0	8	9	
	0	5	0	0	0	known/estimated for some cells and values
	2	4	15	0	19	at unknown cells is zero
	0	0	4	6	0	
(a)						
						1
	6	10	11	9.75	12	Iteration 1: $\frac{1}{4}(0+0+5+15) = 5$
	3	7	6.5	8	9	
	3.75	5	5	2	7	
	2	4	15	10	19	
	1	3	4	6	12.5	
			(b)			
						1
	6	10	11	9.75	12	Iteration 2: $\frac{1}{4}(6.5 + 2 + 5 + 15)$
	3	7	7.75	8	9	= 7.13
	3.75	5	7.13	7.5	8	
	2	4	15	10.5	19	
	2.5	3.25	4	6	12.5	
_						•
			(c)			
	6	10	11	9.75	12	Final Grid with values estimated for all
	3	7	8.79	8	9	
	3.75	5	9.64	10.12	11.93	unknown cells
	2	4	15	12.46	19	
	2.83	3.7	4	6	12.5	
	(d)					

Figure 3. Example of the process for iteration: (a) grid with initial values; (b) grid after first iteration; (c) grid after second iteration; (d) final grid.

Remote Sens. 2023, 15, 3844 8 of 19

2.2. Study Area and Data

Data representing various hydrologic variables at different geographic locations (Figure 4 and Table 1) are used in this study to compare Laplace interpolation with other methods.

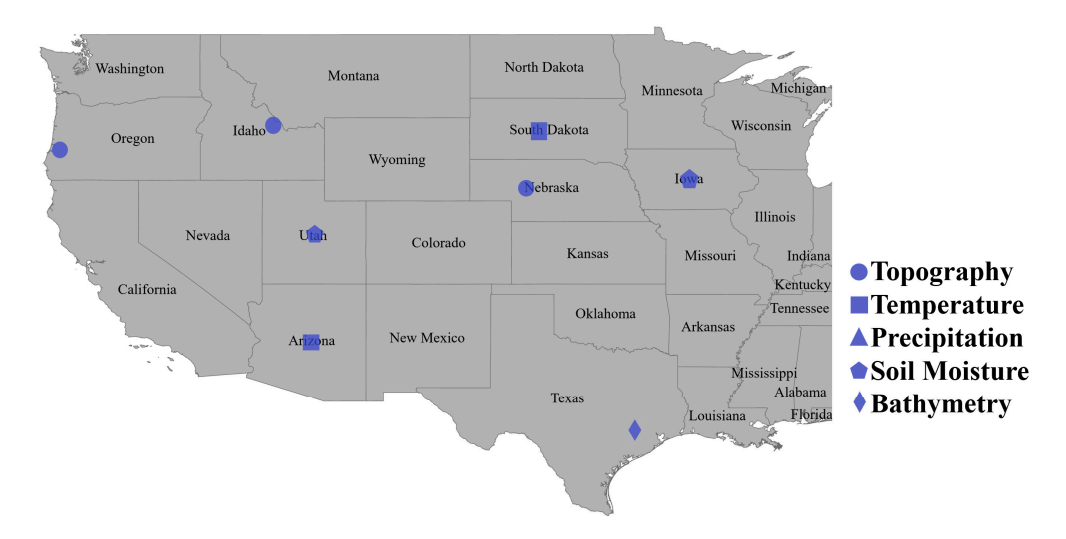


Figure 4. Gauging stations location.

Table 1. Summary of data used for interpolation in this study.

Location	Data Type	Total Points	Area (km²)	Min.	Max.	Mean	SD	Unit
Nebraska	Plain	3291	3.2	946.13	984.55	955.7	6.93	m
Oregon	Coastal area	7475	6.8	129.39	494.08	299.52	80.09	m
Idaho	Mountain	13,230	44.1	2143.54	3079.62	2559.3	213.97	m
South Dakota	Precipitation	184	233,100	211.4	654.5	427.63	92.53	mm/10
Arizona	Precipitation	275	322,400	50.9	535.5	183.17	84.16	mm/10
South Dakota	Temperature	113	233,100	4.5	10.6	8.11	1.28	°C
Arizona	Temperature	135	322,400	6.1	25.1	15.51	4.92	°C
Iowa	Soil moisture	23	141,000	4.15	45.51	29.94	10.42	m^3/m^3
Utah	Soil moisture	33	221,400	1.68	30.22	11.23	6.09	m^3/m^3
Texas	Soil moisture	2453	254,908	0.2	0.42	0.33	0.05	m^3/m^3
New Mexico	Soil moisture	2505	252,477	0.19	0.39	0.23	0.02	m^3/m^3
Brazos river 1	River channel	3529	0.16	4.58	12.06	9.59	1.45	m
Brazos river 2	River channel	3162	0.31	6.84	13.19	11.37	1.16	m
Brazos river 3	River channel	3713	0.2	8.9	13.19	11.4	1.1	m

Notes: SD, standard deviation.

For topography, gridded elevation points from the USGS National Elevation Dataset (USGS, NED, 2020) from three regions representing plains, coastal, or mountainous areas are used (Figure 4). Using a gridded elevation dataset, which is already interpolated, is not ideal. However, considering the overall goal of this study, which is to investigate whether Laplace formulation provides a reasonably simple alternative to other interpolation methods, using an already gridded dataset is assumed to be reasonable. For bathymetry, irregularly spaced survey data points from the Texas Water Development Board (TWDB) for three locations along a reach of the Brazos River in Texas are used. These data were collected using a single-beam boat-mounted acoustic depth sounder linked to a global positioning system [52].

Remote Sens. 2023, 15, 3844 9 of 19

For climate variables, annual precipitation and mean annual temperature datasets in 2020 from the National Oceanic and Atmospheric Administration (NOAA) weather stations are used. Figure 5c,d represents the maps of precipitation and temperature data, respectively. Depth-averaged soil moisture values, which represent the amount of water present in a specific soil layer beneath the surface, are used in this study. Two datasets, representing daily average 12-inch depth soil volumetric water content in 2020 from the Iowa State University soil (ISU) moisture network, and annually averaged 2-inch depth soil moisture at a location in Utah from 2016 to 2020 from the Soil Climate Analysis Network (SCAN), are used. Given the limited number of soil observations from these two sites, data from the Famine Early Warning Systems Network (FEWS NET), and the Land Data Assimilation System (FLDAS) are also utilized in this study. The values of the data with a resolution of 10 km are the average soil moisture in January 2019 from New Mexico, and Texas. The depth of the layer of data in this study is 0 to 10 cm [53]. Besides elevation and the FEWS NET soil data, which are estimates, all other datasets represent field measurements.

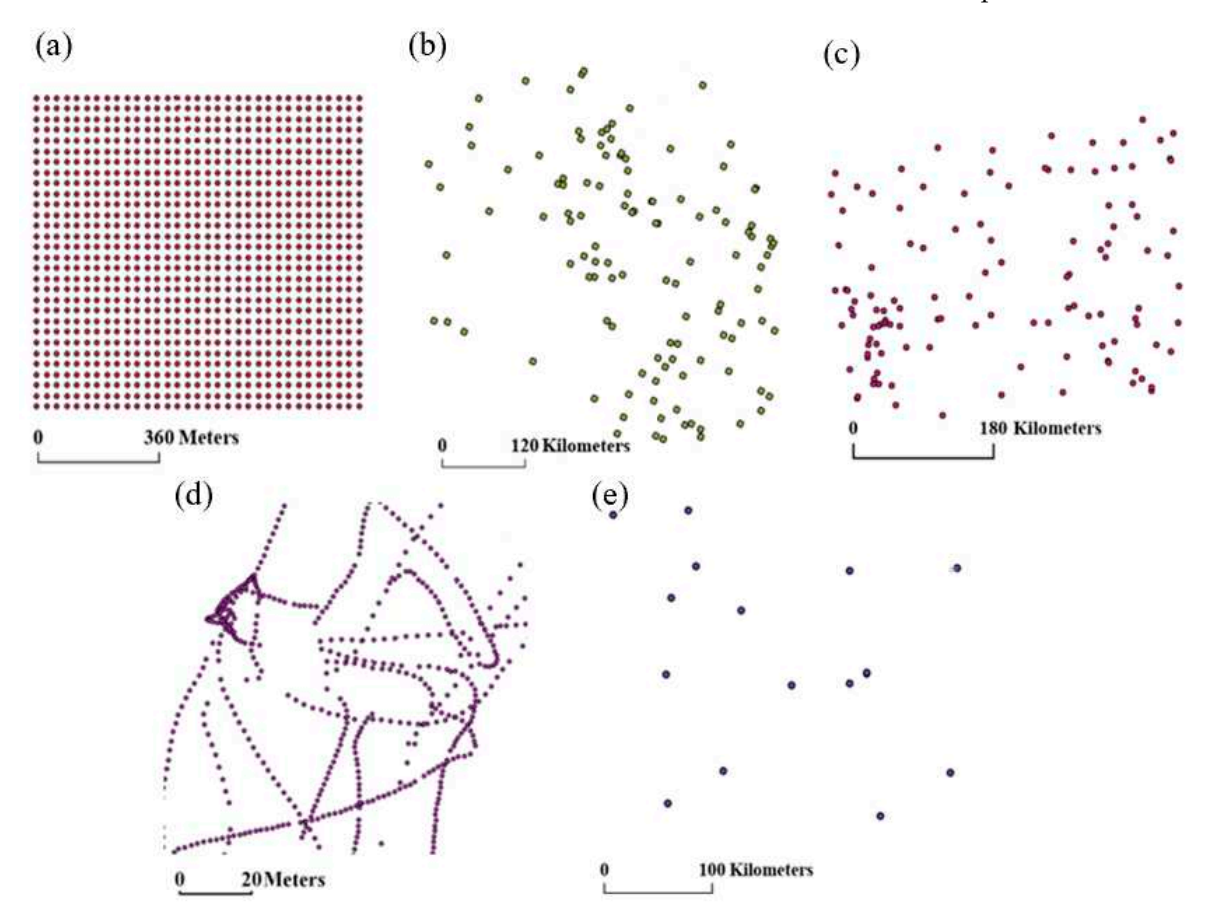


Figure 5. Map of different datasets: (a) topography data in Nebraska; (b) Brazos River bathymetry; (c) precipitation data in South Dakota; (d) temperature data in Arizona; (e) soil moisture data in Iowa.

2.3. Research Methods

The methodology involves the following steps: (1) Data processing to split each dataset into test and validation datasets; (2) interpolating test data using IDW, natural neighbor, Kriging, and LF; and (3) comparing the results from LF with IDW, natural neighbor, and Kriging. The data are randomly separated using a 70/30 split to create testing and validation samples for each dataset. The testing sample is then used for interpolation using the selected methods. Interpolation using IDW, natural neighbor, and kriging is conducted in ArcGIS Pro 2.8.2, and interpolation using Laplace formulation (LF) is coded in Python. The estimates from interpolation using each method are then evaluated using points in the validation sample. This random sampling, interpolation, and validation is repeated

Remote Sens. 2023, 15, 3844 10 of 19

five times to capture the variability in the data and avoid any bias that may result from a single sample. All interpolation methods to create grids or raster surfaces are impacted by the cell size used in creating the final surface [54]. Different cell sizes were used in the present study for each dataset to investigate its impact on the final results. It was found that the performance of each method was consistent among the different cell sizes used, and thus for each dataset, a suitable cell size was chosen to create a representative surface by capturing sufficient information from the testing datasets. Accordingly, a cell size of 30 m and 2 m is used for topography and bathymetry surfaces, respectively. A cell size of 10 km is used for precipitation, temperature, and soil moisture surfaces.

After interpolating each variable using the testing dataset, the interpolated values are compared with values in the validation dataset using RMSE (Equation (18)) and R² (Equation (19)) for quantitative assessment.

RMSE =
$$\sqrt{\frac{\sum_{i=1}^{n} (z_i - \hat{z}_i)^2}{n}}$$
 (18)

where n is the number of points in the validation dataset, z_i and \hat{z}_i is the interpolated value and observed value at point I, respectively.

$$R^2 = 1 - \left(\frac{SS_{res}}{SS_{tot}}\right) \tag{19}$$

where SS_{res} is the sum of squares of residuals, which is the difference between the observed values and predicted values, and SS_{tot} is the total sum of squares, which is the difference between observed values and their mean.

Besides RMSE and R^2 , the interpolated surfaces from each technique are compared visually through differentiation and scatter plots. The methods are also compared in terms of their ease of implementation, including the number of input parameters and computational speed.

3. Results

3.1. Quantitative Assessment

RMSE, R² values, and scatter plots for all techniques using the validation dataset for each sample are presented in Tables 2 and 3, and Figures 6–8, respectively.

	Location	IDW	NN	Kriging	LF	Unit
Topography	Nebraska	1.24	1.06	1	1.08	m
	Oregon	5.77	4.22	4.55	4.24	m
1017	Idaho	4.66	3.54	2.87	3.16	m
Bathymetry	Brazos river 1	0.3	0.25	0.43	0.28	m
	Brazos river 2	0.17	0.13	0.28	0.18	m
	Brazos river 3	0.29	0.22	0.26	0.31	m
Precipitation	Arizona	53.57	53.69	50.87	54.86	mm/10
	South Dakota	61.08	61.58	62.41	58.43	mm/10
Temperature	Arizona	2.55	2.55	2.5	2.47	°C
	South Dakota	0.85	0.81	0.83	0.78	°C
Soil Moisture	Iowa	9.91	7.38	11.08	11.39	%
	Utah	7.35	5.62	7.72	7.58	%
	New Mexico	1.31	1.27	1.36	1.23	%
	Texas	0.87	0.86	0.86	0.85	%

Table 2. Table showing RMSE values from interpolation for all variables.

Remote Sens. 2023, 15, 3844 11 of 19

	Location	IDW	NN	Kriging	LF
	Nebraska	0.97	0.98	0.98	0.98
Topography	Oregon	1.00	1.00	1.00	1.00
1 0 1 7	Idaho	1.00	1.00	1.00	1.00
	Brazos river 1	0.96	0.97	0.92	0.96
Bathymetry	Brazos river 2	0.98	0.99	0.95	0.98
, ,	Brazos river 3	0.97	0.98	0.97	0.97
D ' ' ' '	Arizona	0.94	0.94	0.94	0.93
Precipitation	South Dakota	0.95	0.95	0.95	0.92
T	Arizona	0.92	0.91	0.92	0.91
Temperature	South Dakota	0.95	0.90	0.94	0.92
	Iowa	0.71	0.74	0.70	0.72
0.1114.11	Utah	0.77	0.78	0.76	0.76
Soil Moisture	New Mexico	0.87	0.88	0.86	0.88
	Texas	0.98	0.98	0.98	0.98

Table 3. Table showing R^2 values from interpolation of all variables.

3.1.1. Topography

The increase in RMSE of IDW compared to Laplace formulation (LF) ranges from 0.16 m for the plains to 1.53 m for the coastal dataset. The change in RMSE of LF compared to natural neighbor and kriging is within 0.4 m. The change in R^2 is minimal. Overall, the performance of LF in interpolating topography data is quite comparable to that of natural neighbor and kriging, which is also visible in the scatter plot results (Figure 6).

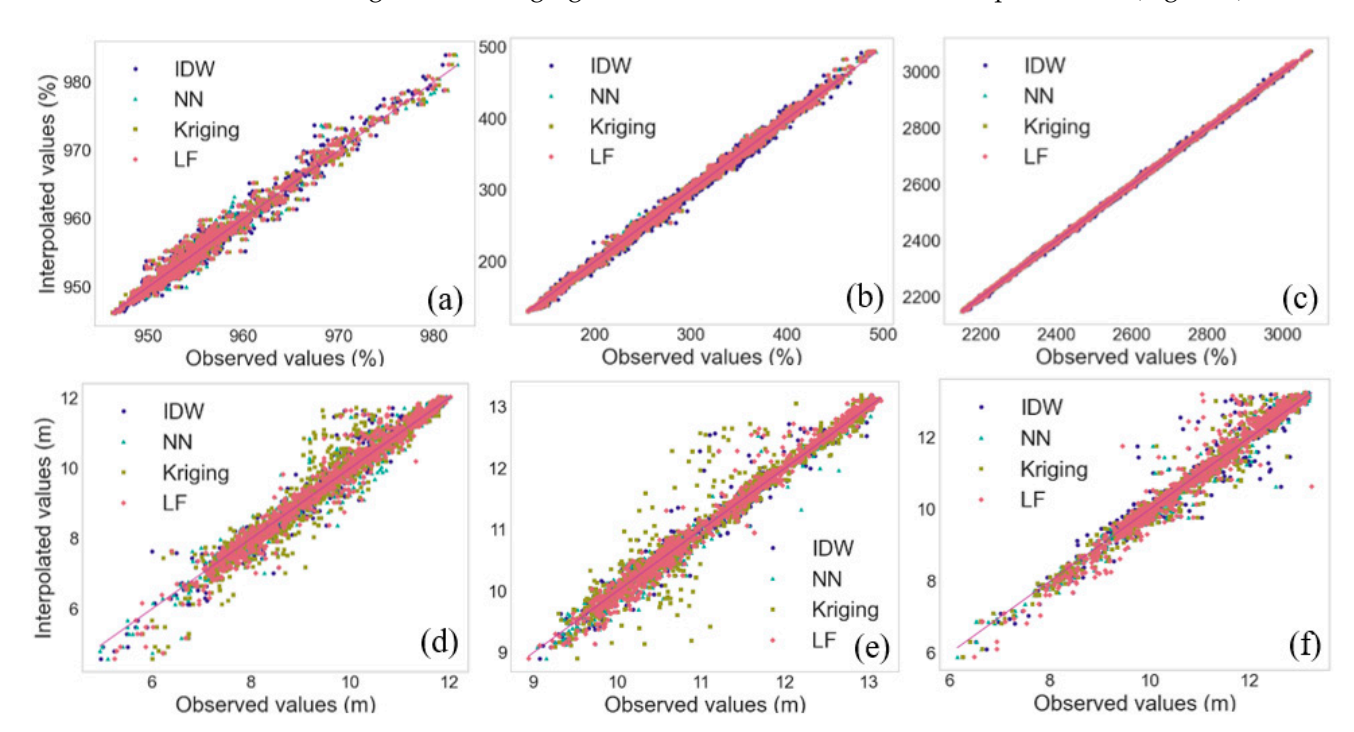


Figure 6. Scatterplot showing the relationship between observation and estimates of different methods for topography data in: (a) Nebraska; (b) Oregon; (c) Idaho, bathymetry data in: (d) Brazos River 1; (e) Brazos River 2; (f) Brazos River 3. The y = x line is utilized to determine the performance of each method.

Remote Sens. 2023, 15, 3844 12 of 19

3.1.2. Bathymetry

Unlike the results for topography data, the change in RMSE for IDW is less than 0.2 m for bathymetry, indicating similar performance between LF and IDW. RMSE results for natural neighbor show a relative decrease from 0.03 m to 0.09 m, which means that natural neighbor performs slightly better than LF. The increases in RMSE of kriging are 0.15 and 0.1 for Brazos River 1 and 2, indicating a better performance of LF compared to kriging. The change in the R² percentage is minimal, within 0.4. Overall, the performance of LF is again comparable to other methods for interpolating bathymetry data. The scatter plots for bathymetry also show an equal spread of over and under estimation for all methods, except for Kriging (Figure 6). The Kriging method under- and overestimated more bathymetry points compared to other methods for Brazos River 1 and 2.

3.1.3. Climate

The change in RMSE for both precipitation and temperature is small for IDW, Kriging, and NN compared to LF. Overall, LF performed better than other methods for the Arizona dataset, but the performance of LF is relatively poorer for the South Dakota dataset, but again, the relative change is smaller than 3.99 mm/10. All three methods exhibited slightly better performance than LF in terms of interpolating temperature data, with a minimal change in RMSE and R². The scatter plots for both precipitation and temperature show an equal spread of overestimation and underestimation for all methods (Figure 7). Overall results show that each method performed similarly, and the accuracy of the prediction for all methods is limited by the relatively smaller number of testing points.

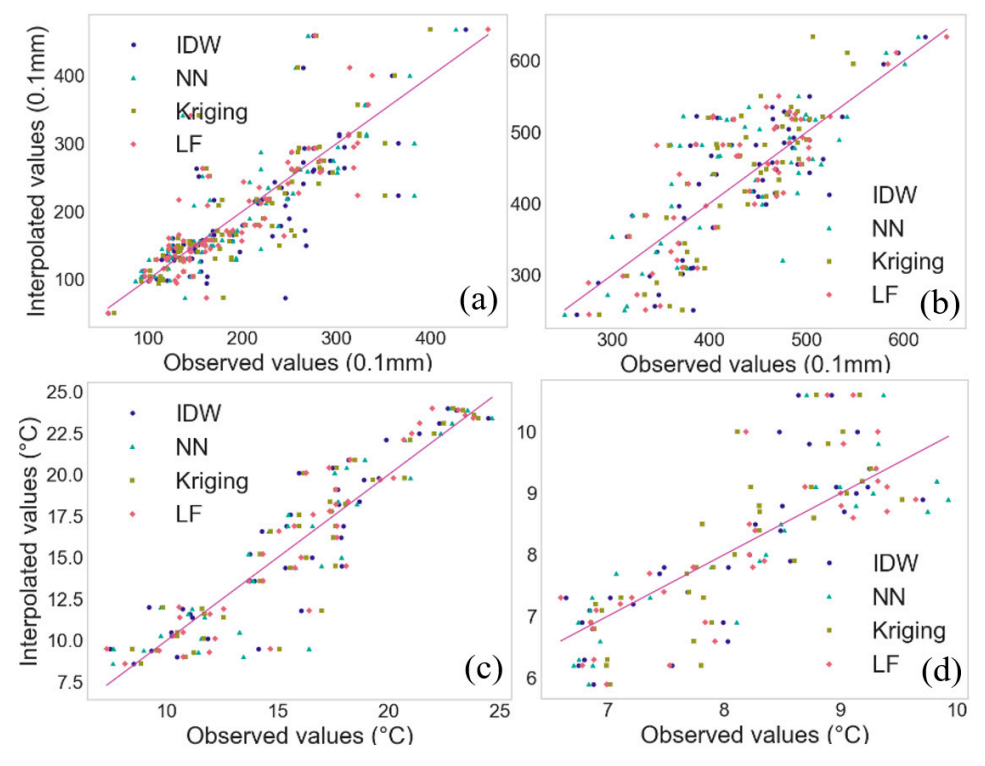


Figure 7. Scatterplot showing the relationship of observation and estimates of different methods for precipitation data in: (a) Arizona; (b) South Dakota, and temperature data in: (c) Arizona; (d) South Dakota. The y = x line is utilized to determine the performance of each method.

3.1.4. Soil Moisture

Interpolation results from soil moisture show that the performance of LF is mixed in terms of RMSE compared to other methods. For example, the RMSE results for LF are similar, but NN outperforms other methods for both datasets in Iowa and Utah. IDW also outperforms Kriging for the Iowa dataset, but the results for Utah are comparable. The

Remote Sens. 2023, 15, 3844 13 of 19

decrease for places that have more observation points ranges from 0.01 to 0.13%, indicating that LF performed slightly better than other methods. It is observed from the scatterplots of soil moisture data in Iowa and Utah that most points are far above or below the identity line. However, the distribution of points for each method in the other two places with more observed data (FEWS NET) is similar (Figure 8). The number of testing points shown in Table 1 is 23 and 33 for Iowa and Utah, respectively. Therefore, the scarcity of testing points causes the inaccurate prediction. This is also the reason that the percentage change in R² in Iowa and Utah is greater than in other places. The number of observation points has a significant impact on the performance of interpolation methods for soil moisture data.

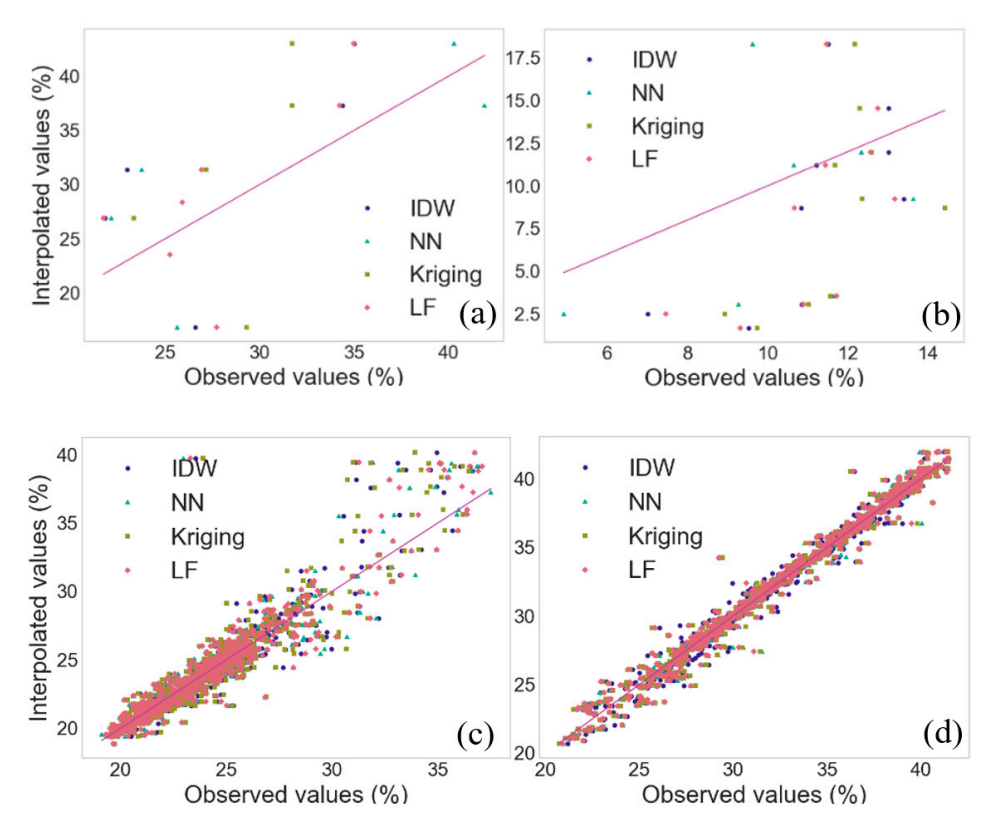


Figure 8. Scatterplot showing the relationship of observation and estimates of different methods for soil moisture data in: (a) Iowa; (b) Utah; (c) New Mexico; (d) Texas. The y = x line is utilized to determine the performance of each method.

3.2. Visual Analysis

Visual analysis helps identify specific issues, such as spikes or depressions in an interpolated surface, that are not easily revealed through quantitative assessment. For this purpose, difference plots, obtained by simply subtracting the base surface from the interpolated surface, are used to analyze the performance of each method. The base surface was created using Kriging to interpolate all observed points, including testing and validation points. Kriging was used because it is reported to perform better than other methods from past studies for interpolating many variables used in hydrology [19,36,55,56]. Overall, the difference plots show that there are no obvious spots or mismatching spatial trends among the interpolated surfaces of precipitation, temperature, and soil data (Figure 9). For bathymetry data, LF underestimates values at some locations along the banks, as indicated by dark areas (circled in Figure 10). Upon inspection, it is found that these locations have relatively fewer testing points than others, and that may have impacted the performance of LF at these locations.

Remote Sens. 2023, 15, 3844 14 of 19

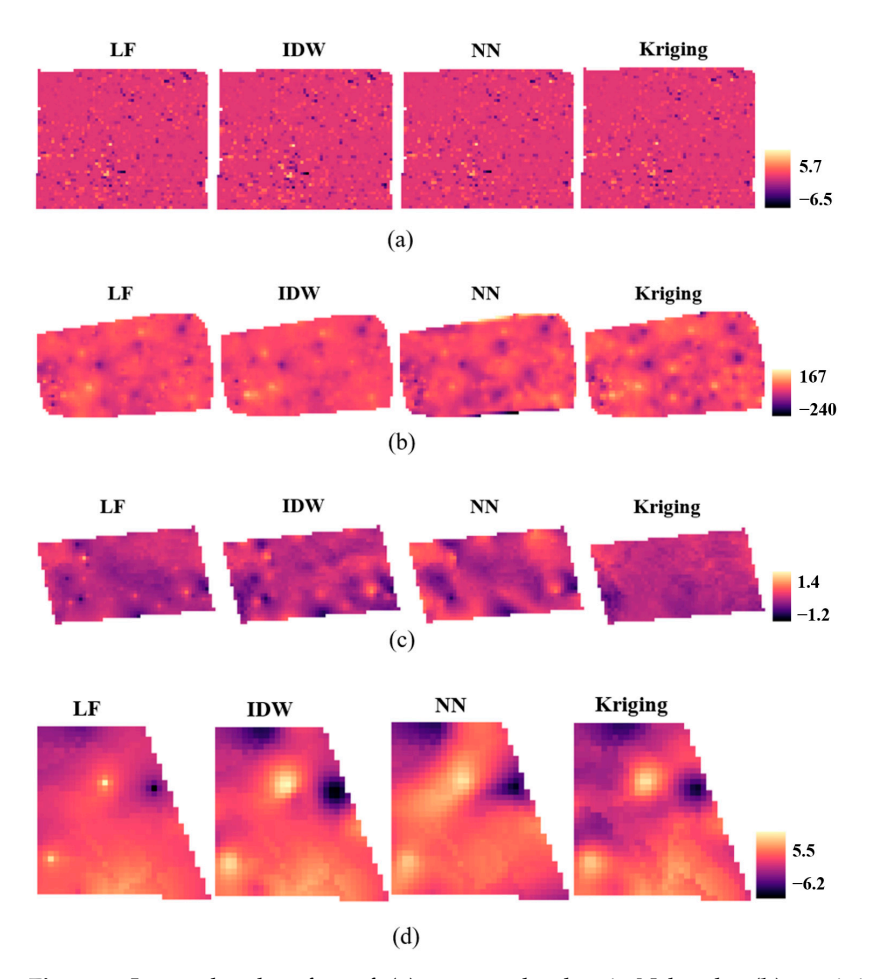


Figure 9. Interpolated surface of: (a) topography data in Nebraska; (b) precipitation data in South Dakota; (c) temperature data in South Dakota; (d) soil moisture data in Utah.

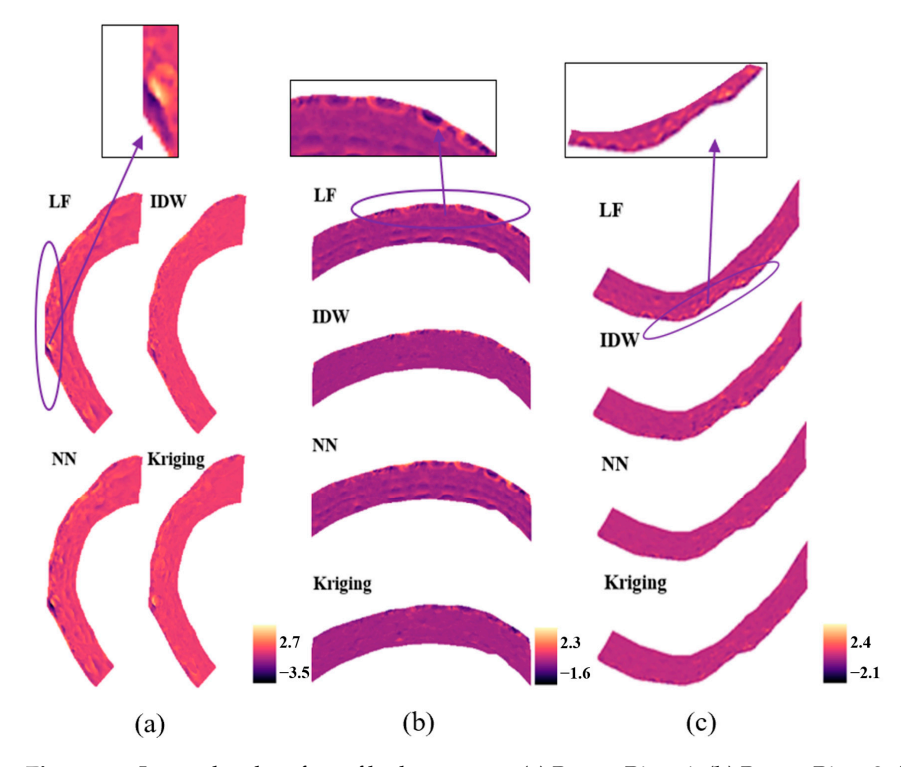


Figure 10. Interpolated surface of bathymetry at: (a) Brazos River 1; (b) Brazos River 2; (c) Brazos River 3.

Remote Sens. 2023, 15, 3844 15 of 19

3.3. Computational Needs

In terms of implementation, natural neighbor does not need any input parameter, LF needs error tolerance, IDW needs both the power (2 is common) and search radius, and Kriging needs input for the semi-variogram model for fitting the data and search radius. Overall, in terms of implementation, Natural neighbor is the easiest, followed by LF, IDW, and Kriging. A comparison of the computational time for all methods shows that the computationally LF is faster for topography, soil, precipitation, and temperature data (see Table 4). For bathymetry data, LF is much slower compared to other methods. The main factor that affected the computational results for LF was the smaller cell size of 2 m for bathymetry points. Table 5 presents the results of the computational time for a finer size, revealing that LF is considerably slower in comparison to other methods. This is due to the fact that a smaller cell size leads to an increase in the number of unknown points that require computation, resulting in a slower overall computational speed.

Table 4. Computational time for all data in second.

	IDW	NN	Kriging	LF	Cell Size (m)
Topography	1.03	1.19	1.45	0.91	30
Soil moisture	1.32	0.90	0.95	0.18	10^{4}
Precipitation	1.11	0.80	0.84	0.31	10^{4}
Temperature	1.07	0.77	0.79	0.22	10^{4}
Bathymetry	1.14	1.27	1.30	5.36	2

Table 5. Computational time for all data in second for finer cell size.

	IDW	NN	Kriging	LF	Cell Size (m)
Topography	1.41	1.28	2.46	65.95	5
Soil moisture	2.13	2.1	2.89	9.84	500
Precipitation	1.14	0.95	1.03	0.53	500
Temperature	1.15	0.93	1.06	0.65	500
Bathymetry	1.41	2.5	2.21	54.47	1

In addition, smaller tolerances would result in slower computational speed for LF because smaller tolerances require more iterations to reach convergence. For example, the running time of LF is 5.4, 16.8, and 27.9 s using tolerances of 0.001, 0.0001, and 0.00001 m to interpolate bathymetry data of Brazos River 1, respectively. Kriging is computationally more intensive compared to other methods [39,57], which, however, is not found in the present study. The number of points in different datasets is only several thousand or less, as shown in Table 1, indicating that the relatively small data size can be the reason why the computational speed of every method is quite comparable.

4. Discussion and Conclusions

The main objective of this study is to assess the applicability of the Laplace Formulation (LF) for interpolating hydrologic data, which has been sparsely explored in previous literature, with only two known studies by Hess [43] and Lai [44] utilizing this approach. Unlike commonly used methods such as inverse distance weighting (IDW), natural neighbor (NN), and Kriging that rely on distance or area-based weighting, LF is based on the spatial behavior of surrounding points. Specifically, it tries to maintain the smoothness or surface curvature based on surrounding points. The objective of this study is accomplished by interpolating different types of hydrologic data from diverse regions using the LF method. The interpolated results are then quantitatively and qualitatively compared to those obtained using IDW, NN, and Kriging. The evaluation, based on RMSE and R², revealed that LF produced interpolated values for topography data that are comparable to the other methods. Specifically, its RMSE values are close to those of Kriging and NN, and it outperformed IDW. These findings align with those of Arun [58]. Kriging considers

Remote Sens. 2023, 15, 3844 16 of 19

autocorrelation in elevations, enabling the determination of optimal weights, and NNs generate a smooth estimated surface, except for points with discontinuous derivatives [59]. LF, which also attempts to create a smooth surface, performed similarly to Kriging and NN. Scatterplots and corresponding R² values depicting the relationship between observations and estimates indicated similar performance among the techniques for estimating topography data.

With respect to bathymetry data, LF yielded RMSE results comparable to those of NN and IDW. However, upon examining the difference plots, it was observed that LF tended to underestimate values along the riverbanks, where data points were relatively sparse. Previous studies have suggested that Kriging is a more suitable interpolator for bathymetry data [37,60-62]. In this specific case, the limited availability of data points along the riverbanks of the Brazos River 1 and 2 contributed to the poorer performance of Kriging. For precipitation data, LF demonstrated slightly better performance than other methods in Arizona but slightly poorer performance in South Dakota. This difference can be explained by the variability in the precipitation data in these regions. The precipitation data for South Dakota have a slightly higher standard deviation (92.53 mm/10) compared to that of Arizona (84.16 mm/10). This may affect the LF, given its property of creating a smoother surface. However, it is difficult to generalize this given the limited datasets used in this study. Additionally, the difference in RMSE results, within 4 mm of precipitation, is not outside the variability observed among RMSE from all methods. Studies have shown that the performance of different interpolation methods varies across different locations. Ordinary Kriging is generally considered a superior method for interpolation precipitation, but some studies have found that IDW can produce similar results compared to Kriging [22,63,64].

For temperature data, previous studies have suggested that IDW is the most suitable method [65,66]. The lack of observational data points in this study may explain why all methods yielded similar performance. The results for soil data varied across the methods for the four regions used in this study. Except for Iowa, LF performance is comparable to all other methods. Even for Iowa, its RMSE results are close to those of Kriging but higher than those of IDW and NN. Similar to precipitation data, the relative poorer performance of LF for the Iowa region can be attributed to the higher variance in the data. However, there may be other factors playing a role in the overall performance. According to previous studies, when the land is complex, IDW and ordinary Kriging are not recommended due to the low spatial autocorrelation of soil moisture [33,67]. All the locations analyzed in this study had diverse landscapes across the states, with different types of land cover and topography.

Computational speed analysis revealed that LF performed similarly to the other methods for most sample datasets in this study, but its performance was adversely affected as the number of data points increased. While all interpolation results were computed using the Python environment, it should be noted that there are packages available for other methods that may be optimized for computational efficiency. The current code for LF that is implemented in this study needs further work to improve its efficiency. Specifically, the role of spatial configuration, including regular versus irregular spacing of data points, spatial density, and sample size, requires a more comprehensive investigation. These factors can potentially affect the accuracy and reliability of LF interpolation. While this study identified data size and error tolerance as potential challenges for LF, these issues can be mitigated by parallelizing the code, thus facilitating future studies and applications.

The overall goal of this study was to propose LF as a simpler approach to commonly used existing methods and evaluate its performance. In conclusion, the findings suggest that LF offers a viable alternative for interpolating hydrologic variables, providing comparable results to commonly used methods such as IDW, NN, and Kriging. LF offers the advantage of simpler implementation and reduced user input requirements. However, careful consideration is required when using LF for datasets with sparse data points or high computational demands. Interpolation methods are often used by practitioners to process and prepare data for input into hydrologic analyses and models. The literature suggests

Remote Sens. 2023, 15, 3844 17 of 19

using different methods for interpolating different variables. Often, these methods provide the best results when the choice of parameters, such as search radius, distance or area weights, and semi-variogram type, associated with their implementation is correct. In the absence of background knowledge about different methods, practitioners use the default settings, which may or may not provide the best results. The simple LF formulation does not involve the selection of any parameters and avoids subjectivity in its implementation, thus providing a simpler and more robust alternative to existing methods. In addition, LF offers an interesting path for researchers because of its theoretical background in hydrology. It is used in hydrology for describing flow fields (flownet), and what this study shows is that it may be suitable for creating or describing other scalar fields in hydrology.

Author Contributions: Conceptualization, T.X. and V.M.; methodology, T.X.; software, T.X. and Z.W.; validation, T.X. and Z.W.; formal analysis, T.X.; resources, T.X.; writing—original draft preparation, T.X.; writing—review and editing, T.X. and V.M.; visualization, T.X.; supervision, V.M. All authors have read and agreed to the published version of the manuscript.

Funding: This research was partially funded by the U.S. National Science Foundation (Award: 2033607).

Data Availability Statement: Python code and the hydrologic data used in the present study can be found in HydroShare: http://www.hydroshare.org/resource/d889155d1fbd4fe38495dc0f140d83a4 (accessed on 28 July 2023).

Conflicts of Interest: The authors declare no conflict of interest.

References

 Nijssen, B.; Lettenmaier, D.P. Effect of precipitation sampling error on simulated hydrological fluxes and states: Anticipating the Global Precipitation Measurement satellites. J. Geophys. Res. Atmos. 2004, 109, D02103. [CrossRef]

- 2. Pan, M.; Li, H.; Wood, E. Assessing the skill of satellite-based precipitation estimates in hydrologic applications. *Water Resour. Res.* **2010**, *46*, W09535. [CrossRef]
- 3. Seneviratne, S.I.; Corti, T.; Davin, E.L.; Hirschi, M.; Jaeger, E.B.; Lehner, I.; Orlowsky, B.; Teuling, A.J. Investigating soil moisture—Climate interactions in a changing climate: A review. *Earth-Sci. Rev.* **2010**, *99*, 125–161. [CrossRef]
- 4. Brocca, L.; Morbidelli, R.; Melone, F.; Moramarco, T. Soil moisture spatial variability in experimental areas of central Italy. *J. Hydrol.* **2007**, 333, 356–373. [CrossRef]
- 5. Wagner, W.; Blöschl, G.; Pampaloni, P.; Calvet, J.-C.; Bizzarri, B.; Wigneron, J.-P.; Kerr, Y. Operational readiness of microwave remote sensing of soil moisture for hydrologic applications. *Hydrol. Res.* **2007**, *38*, 1–20. [CrossRef]
- 6. Habtezion, N.; Nasab, M.T.; Chu, X. How does DEM resolution affect microtopographic characteristics, hydrologic connectivity, and modelling of hydrologic processes? *Hydrol. Process.* **2016**, *30*, 4870–4892. [CrossRef]
- 7. Zhang, W.; Montgomery, D.R. Digital elevation model grid size, landscape representation, and hydrologic simulations. *Water Resour. Res.* **1994**, *30*, 1019–1028. [CrossRef]
- 8. Seo, S.; Das Bhowmik, R.; Sankarasubramanian, A.; Mahinthakumar, G.; Kumar, M. The role of cross-correlation between precipitation and temperature in basin-scale simulations of hydrologic variables. *J. Hydrol.* **2019**, 570, 304–314. [CrossRef]
- 9. Zhao, H.; Yang, S.; Wang, Z.; Zhou, X.; Luo, Y.; Wu, L. Evaluating the suitability of TRMM satellite rainfall data for hydrological simulation using a distributed hydrological model in the Weihe River catchment in China. *J. Geogr. Sci.* **2015**, 25, 177–195. [CrossRef]
- 10. Houser, P.R.; Shuttleworth, W.J.; Famiglietti, J.S.; Gupta, H.V.; Syed, K.H.; Goodrich, D.C. Integration of soil moisture remote sensing and hydrologic modeling using data assimilation. *Water Resour. Res.* **1998**, *34*, 3405–3420. [CrossRef]
- 11. Mattia, F.; Satalino, G.; Pauwels, V.R.N.; Loew, A. Soil moisture retrieval through a merging of multi-temporal L-band SAR data and hydrologic modelling. *Hydrol. Earth Syst. Sci.* **2009**, *13*, 343–356. [CrossRef]
- 12. Azimi, S.; Dariane, A.B.; Modanesi, S.; Bauer-Marschallinger, B.; Bindlish, R.; Wagner, W.; Massari, C. Assimilation of Sentinel 1 and SMAP—Based satellite soil moisture retrievals into SWAT hydrological model: The impact of satellite revisit time and product spatial resolution on flood simulations in small basins. *J. Hydrol.* 2020, 581, 124367. [CrossRef] [PubMed]
- 13. Jiang, D.; Wang, K. The role of satellite-based remote sensing in improving simulated streamflow: A review. *Water* **2019**, *11*, 1615. [CrossRef]
- 14. Corbari, C.; Mancini, M.; Li, J.; Su, Z. Can satellite land surface temperature data be used similarly to river discharge measurements for distributed hydrological model calibration? *Hydrol. Sci. J.* **2015**, *60*, 202–217. [CrossRef]
- 15. Chen, H.; Fan, L.; Wu, W.; Liu, H.B. Comparison of spatial interpolation methods for soil moisture and its application for monitoring drought. *Environ. Monit. Assess.* **2017**, *189*, 525. [CrossRef]

Remote Sens. 2023, 15, 3844 18 of 19

16. Di Piazza, A.; Conti, F.L.; Noto, L.; Viola, F.; La Loggia, G. Comparative analysis of different techniques for spatial interpolation of rainfall data to create a serially complete monthly time series of precipitation for Sicily, Italy. *Int. J. Appl. Earth Obs. Geoinf.* **2011**, 13, 396–408. [CrossRef]

- 17. Hevesi, J.A.; Istok, J.D.; Flint, A.L. Precipitation Estimation in mountainous terrain using multivariate geostatistics. Part I: Structural analysis. *J. Appl. Meteorol.* **1992**, *31*, 661–676. [CrossRef]
- 18. Hofierka, J.; Parajka, J.; Mitasova, H.; Mitas, L. Multivariate interpolation of precipitation using regularized spline with tension. *Trans. GIS* **2002**, *6*, 135–150. [CrossRef]
- 19. Xu, W.; Zou, Y.; Zhang, G.; Linderman, M. A comparison among spatial interpolation techniques for daily rainfall data in Sichuan Province, China. *Int. J. Clim.* **2015**, *35*, 2898–2907. [CrossRef]
- 20. Larson, L.W.; Peck, E.L. Accuracy of precipitation measurements for hydrologic modeling. *Water Resour. Res.* **1974**, *10*, 857–863. [CrossRef]
- 21. Hutchinson, M.F. Interpolating mean rainfall using thin plate smoothing splines. Int. J. Geogr. Inf. Sci. 1995, 9, 385–403. [CrossRef]
- 22. Ly, S.; Charles, C.; Degre, A. Different methods for spatial interpolation of rainfall data for operational hydrological modeling at watershed scale. A review. *Biotechnol. Agron. Soc. Environ.* **2013**, 17, 392–406. [CrossRef]
- 23. Bell, V.A.; Moore, R.J. The sensitivity of catchment runoff models to rainfall data at different spatial scales. *Hydrol. Earth Syst. Sci.* **2000**, *4*, 653–667. [CrossRef]
- 24. Goudenhoofdt, E.; Delobbe, L. Evaluation of radar-gauge merging methods for quantitative precipitation estimates. *Hydrol. Earth Syst. Sci.* **2009**, *13*, 195–203. [CrossRef]
- 25. Beck, H.E.; van Dijk, A.I.; Levizzani, V.; Schellekens, J.; Miralles, D.G.; Martens, B.; de Roo, A. MSWEP: 3-hourly 0.25° global gridded precipitation (1979–2015) by merging gauge, satellite, and reanalysis data. *Hydrol. Earth Syst. Sci.* **2017**, 21, 589–615. [CrossRef]
- 26. Schiemann, R.; Erdin, R.; Willi, M.; Frei, C.; Berenguer, M.; Sempere-Torres, D. Geostatistical radar-raingauge combination with nonparametric correlograms: Methodological considerations and application in Switzerland. *Hydrol. Earth Syst. Sci.* **2011**, *15*, 1515–1536. [CrossRef]
- 27. Amini, M.A.; Torkan, G.; Eslamian, S.; Zareian, M.J.; Adamowski, J.F. Analysis of deterministic and geostatistical interpolation techniques for mapping meteorological variables at large watershed scales. *Acta Geophys.* **2018**, *67*, 191–203. [CrossRef]
- 28. Apaydin, H.; Sonmez, F.K.; Yildirim, Y.E. Spatial interpolation techniques for climate data in the GAP region in Turkey. *Clim. Res.* **2004**, *28*, 31–40. [CrossRef]
- 29. Musashi, J.P.; Pramoedyo, H.; Fitriani, R. Comparison of inverse distance weighted and natural neighbor interpolation method at air temperature data in malang region. *CAUCHY* **2018**, *5*, 48–54. [CrossRef]
- 30. Di Piazza, A.; Conti, F.L.; Viola, F.; Eccel, E.; Noto, L.V. Comparative analysis of spatial interpolation methods in the Mediterranean area: Application to temperature in Sicily. *Water* **2015**, *7*, 1866–1888. [CrossRef]
- 31. Wang, M.; He, G.; Zhang, Z.; Wang, G.; Zhang, Z.; Cao, X.; Wu, Z.; Liu, X. Comparison of spatial interpolation and regression analysis models for an estimation of monthly near Surface Air Temperature in China. *Remote Sens.* **2017**, *9*, 1278. [CrossRef]
- 32. Vicente-Serrano, S.M.; Saz-Sánchez, M.A.; Cuadrat, J.M. Comparative analysis of interpolation methods in the middle Ebro Valley (Spain): Application to annual precipitation and temperature. *Clim. Res.* **2003**, 24, 161–180. [CrossRef]
- 33. Yao, X.; Fu, B.; Lü, Y.; Sun, F.; Wang, S.; Liu, M. Comparison of four spatial interpolation methods for estimating soil moisture in a complex terrain catchment. *PLoS ONE* **2013**, *8*, e54660. [CrossRef]
- 34. Arseni, M.; Voiculescu, M.; Georgescu, L.P.; Iticescu, C.; Rosu, A. Testing different interpolation methods based on single beam Echosounder River Surveying. case study: Siret river. *ISPRS Int. J. Geo-Inf.* **2019**, *8*, 507. [CrossRef]
- 35. Batista, P.V.G.; Silva, M.L.N.; Avalos, F.A.P.; De Oliveira, M.S.; De Menezes, M.D.; Curi, N. Hybrid kriging methods for interpolating sparse River Bathymetry Point Data. *Ciênc. Agrotecnol.* **2017**, *41*, 402–412. [CrossRef]
- 36. Merwade, V.M.; Maidment, D.R.; Goff, J.A. Anisotropic considerations while interpolating river channel bathymetry. *J. Hydrol.* **2006**, *331*, 731–741. [CrossRef]
- 37. Wu, C.-Y.; Mossa, J.; Mao, L.; Almulla, M. Comparison of different spatial interpolation methods for historical hydrographic data of the lowermost Mississippi River. *Ann. GIS* **2019**, 25, 133–151. [CrossRef]
- 38. Panhalkar, S.S.; Jarag, A.P. Assessment of spatial interpolation techniques for river bathymetry generation of Panchganga River basin using geoinformatic techniques. *Asian J. Geoinform.* **2016**, *15*, 10–15.
- 39. Gentile, M.; Courbin, F.; Meylan, G. Interpolating Point Spread Function Anisotropy. Astron. Astrophys. 2012, 549, A1. [CrossRef]
- 40. Briggs, I.C. Machine contouring using minimum curvature. Geophysics 1974, 39, 39–48. [CrossRef]
- 41. Grain, I. Computer interpolation and contouring of two-dimensional data: A review. Geoexploration 1970, 8, 71–86. [CrossRef]
- 42. Watson, D. Contouring: A Guide to the Analysis and Display of Spatial Data; Elsevier: Amsterdam, The Netherlands, 2013.
- 43. Hess, K.W. Spatial interpolation of tidal data in irregularly-shaped coastal regions by numerical solution of Laplace's equation. *Estuar. Coast. Shelf Sci.* **2002**, *54*, 175–192. [CrossRef]
- 44. Lai, R.; Wang, M.; Yang, M.; Zhang, C. Method based on the Laplace equations to reconstruct the river terrain for two-dimensional hydrodynamic numerical modeling. *Comput. Geosci.* **2018**, *111*, 26–38. [CrossRef]
- 45. Watson, D.F.; Phillip, G.M. Neighbor-Based Interpolation: Geobyte; Pergamon: Oxford, UK, 1987; pp. 12–16.
- 46. Sibson, R. A brief description of natural neighbour interpolation. In *Interpret. Multivar. Data*; John Wiley & Sons: Hoboken, NJ, USA, 1981; pp. 21–26.

Remote Sens. 2023, 15, 3844 19 of 19

47. Oliver, M.A.; Webster, R. Kriging: A method of interpolation for Geographical Information Systems. *Int. J. Geogr. Inf. Sci.* **1990**, *4*, 313–332. [CrossRef]

- 48. Cressie, N. The origins of kriging. Math. Geol. 1990, 22, 239–252. [CrossRef]
- 49. McBRATNEY, A.B.; Webster, R. Choosing functions for semi-variograms of soil properties and fitting them to sampling estimates. *J. Soil Sci.* **1986**, 37, 617–639. [CrossRef]
- 50. López-Acosta, N.P. Numerical and analytical methods for the analysis of flow of water through soils and earth structures. In *Groundwater—Contaminant and Resource Management*; IntechOpen: London, UK, 2016. [CrossRef]
- 51. Shaw, F.S.; Southwell, R.V. Relaxation methods applied to engineering problems. VII. Problems relating to the percolation of fluids through porous materials. *Proc. R. Soc. Lond. Ser. A Math. Phys. Sci.* **1941**, 178, 1–17. [CrossRef]
- 52. Merwade, V. Effect of spatial trends on interpolation of river bathymetry. J. Hydrol. 2009, 371, 169–181. [CrossRef]
- 53. McNally, A. *FLDAS Noah Land Surface Model L4 Global Monthly 0.1* × *0.1 Degree (MERRA-2 and CHIRPS)*; Goddard Earth Sciences Data and Information Services Center (GES DISC): Greenbelt, MD, USA, 2018.
- 54. Bater, C.W.; Coops, N.C. Evaluating error associated with lidar-derived DEM interpolation. *Comput. Geosci.* **2009**, *35*, 289–300. [CrossRef]
- 55. Laslett, G.M. Kriging and splines: An empirical comparison of their predictive performance in some applications. *J. Am. Stat. Assoc.* **1994**, *89*, 391–400. [CrossRef]
- 56. Li, J.; Heap, A.D. A review of comparative studies of spatial interpolation methods in Environmental Sciences: Performance and impact factors. *Ecol. Inform.* **2011**, *6*, 228–241. [CrossRef]
- 57. Longley, P.A.; Goodchild, M.F.; Maguire, D.J.; Rhind, D.W. *Geographic Information Systems and Science*; John Wiley & Sons: Hoboken, NJ, USA, 2015.
- 58. Arun, P. A comparative analysis of different DEM interpolation methods. *Egypt. J. Remote Sens. Space Sci.* **2013**, *16*, 133–139. [CrossRef]
- 59. Li, J.; Heap, A.D. Spatial interpolation methods applied in the environmental sciences: A review. *Environ. Model. Softw.* **2014**, 53, 173–189. [CrossRef]
- 60. Li, Z.; Peng, Z.; Zhang, Z.; Chu, Y.; Xu, C.; Yao, S.; García-Fernández, F.; Zhu, X.; Yue, Y.; Levers, A.; et al. Exploring modern bathymetry: A comprehensive review of data acquisition devices, model accuracy, and interpolation techniques for enhanced underwater mapping. Front. Mar. Sci. 2023, 10, 1178845. [CrossRef]
- 61. Curtarelli, M.; Leão, J.; Ogashawara, I.; Lorenzzetti, J.; Stech, J. Assessment of spatial interpolation methods to map the bathymetry of an amazonian hydroelectric reservoir to aid in decision making for water management. *ISPRS Int. J. Geo-Inf.* **2015**, *4*, 220–235. [CrossRef]
- 62. Šiljeg, A.; Lozić, S.; Šiljeg, S. A comparison of interpolation methods on the basis of data obtained from a bathymetric survey of Lake Vrana, Croatia. *Hydrol. Earth Syst. Sci.* **2015**, *19*, 3653–3666. [CrossRef]
- 63. Dirks, K.; Hay, J.; Stow, C.; Harris, D. High-resolution studies of rainfall on Norfolk Island: Part II: Interpolation of rainfall data. *J. Hydrol.* 1998, 208, 187–193. [CrossRef]
- 64. Mair, A.; Fares, A. Comparison of rainfall interpolation methods in a mountainous region of a tropical island. *J. Hydrol. Eng.* **2011**, 16, 371–383. [CrossRef]
- 65. Kusuma, D.W.; Murdimanto, A.; Sukresno, B.; Jatisworo, D. Comparison of interpolation methods for sea surface temperature data. *JFMR-J. Fish. Mar. Res.* **2018**, 2, 103–115. [CrossRef]
- 66. Hadi, S.J.; Tombul, M. Comparison of spatial interpolation methods of precipitation and temperature using multiple integration periods. *J. Indian Soc. Remote Sens.* **2018**, *46*, 1187–1199. [CrossRef]
- 67. Srivastava, P.K.; Pandey, P.C.; Petropoulos, G.P.; Kourgialas, N.N.; Pandey, V.; Singh, U. GIS and remote sensing aided information for soil moisture estimation: A comparative study of interpolation techniques. *Resources* **2019**, *8*, 70. [CrossRef]

Disclaimer/Publisher's Note: The statements, opinions and data contained in all publications are solely those of the individual author(s) and contributor(s) and not of MDPI and/or the editor(s). MDPI and/or the editor(s) disclaim responsibility for any injury to people or property resulting from any ideas, methods, instructions or products referred to in the content.